

## Dynamic Spin Label Study of the Barstar–Barnase Complex

V. P. Timofeev<sup>1\*</sup>, T. G. Balandin<sup>2</sup>, Ya. V. Tkachev<sup>1</sup>, V. V. Novikov<sup>1</sup>, V. A. Lapuk<sup>3</sup>, and S. M. Deev<sup>2</sup>

<sup>1</sup>Engelhardt Institute of Molecular Biology, Russian Academy of Sciences, ul. Vavilova 32, 119991 Moscow, Russia; fax: (495) 135-1405; E-mail: tim@eimb.ru

<sup>2</sup>Shemyakin and Ovchinnikov Institute of Bioorganic Chemistry, Russian Academy of Sciences, ul. Miklukho-Maklaya 16/10, 117997 Moscow, Russia; E-mail: deev@ibch.ru

<sup>3</sup>Zelinsky Institute of Organic Chemistry, Russian Academy of Sciences, Leninsky pr. 47, 117913 Moscow, Russia; E-mail: lapuk@ioc.ac.ru

Received January 30, 2007

Revision received April 13, 2007

**Abstract**—The dynamic spin label method was used to study protein–protein interactions in the model complex of the enzyme barnase (Bn) with its inhibitor barstar. The C40A mutant of barstar (Bs) containing a single cysteine residue was modified with two different spin labels varying in length and structure of a flexible linker. Each spin label was selectively bound to the Cys82 residue, located near the Bn–Bs contact site. The formation of the stable protein complex between Bn and spin labeled Bs was accompanied by a substantial restriction of spin label mobility, indicated by remarkable changes in the registered EPR spectra. Order parameter,  $S$ , as an estimate of rapid reorientation of spin label relative to protein molecule, was sharply increasing approaching 1. However, the rotational correlation time  $\tau$  for spin-labeled Bs and its complex with Bn in solution corresponded precisely to their molecular weights. These data indicate that both Bs and its complex with Bn are rigid protein entities. Spin labels attached to Bs in close proximity to an interface of interaction with Bn, regardless of its structure, undergo significant restriction of mobility by the environment of the contact site of the two proteins. The results show that this approach can be used to investigate fusion proteins containing Bn or Bs.

DOI: 10.1134/S0006297907090118

**Key words:** mutant spin-labeled barstar, barnase, spin label, EPR spectra of protein complex, order parameter, correlation time

Protein–protein interactions are of interest as a basis for the recognition of many biological structures [1]. A number of questions emerge; one is the estimation of mobility of side-chain residues in the contact site of two interacting globular protein structures. Spatial restriction of mobility of side-chain groups in the contact site region of a protein should substantially depend upon the formation of a complex. There are many methods for monitoring protein interaction: X-ray structural analysis, NMR, fluorescence, light scattering, ultracentrifugation, etc. The spin label method [2] in our modification [3] is successfully used in the present work. This study addressed

the barnase (Bn)–barstar (Bs) protein complex, which is a very tight entity used for the development of sophisticated multivalent protein complexes [4]. We used mutant barstar (Bs), where cysteine residue C40 located in the Bn contact region was replaced by alanine [5]. As a result of this substitution, which does not substantially affect complex stability [5], the only cysteine remaining in the Bs molecule is in position 82. This residue positioned at the border of the Bn–Bs complex contact region is localized at the surface of the protein globule, and thus it is accessible for modification. The thiol group of this residue was used to selectively attach spin labels. Two spin labels were used, whose structural differences provided higher (SL2) or lower (SL1) accessibility of the reporter group to different protein microenvironments. The incorporation of spin label did not hinder the formation of the tight Bn–Bs complex. We found that the mobility (or more exactly the rapid angular reorientation of the nitroxyl radical) of spin label attached to residue C82 of Bs was considerably restrained in the complex compared to the mobility of the spin label in monomeric Bs. The restriction of mobility

**Abbreviations:** Bn) barnase; Bs) mutant C40A barstar; Bs-SL1, Bs-SL2) spin labeled Bs; Bs-SL1–Bn, Bs-SL2–Bn) complexes of spin-labeled Bs and Bn; BOPs) broad outer peaks on EPR spectra; SL1) spin label 3-(2-maleimidoethylcarbamoyl)-2,2,5,5-tetramethylpyrrolidine-1-oxyl; SL2) spin label 4-(2-chloromercuriphenyl)-2,2,5,5-tetramethyl-3-imidazoline- $\Delta^3$ -1-oxyl; SFS) superfine structure.

\* To whom correspondence should be addressed.

was observed for both spin labels despite their structural differences.

For quantitative assessment of the mobility of the spin-labeled C82 side-chain group and of the whole protein globule, the dynamic spin label method [6–8] based on the changes in EPR spectra of spin labeled samples as a function of medium viscosity at constant temperature was applied. An increase in medium viscosity causes broad outer peaks (BOPs) of increasing amplitude to appear on EPR spectra in the low- and high-field regions. Processing of a series of EPR spectra of spin labeled samples includes measurement of distance between BOPs, an assessment of effective rotational correlation time  $\tau$  for the protein molecule, and order parameter  $S$  for the side chain spin label [3, 9]. According to the Stokes–Einstein law, parameter  $\tau$  is proportional to the molecular weight of the spin label carrier (protein globule), and parameter  $S$  is proportional to the spatial limitations of fast angular reorientation of the spin label by the proximal protein environment.

The goal of the present work was to determine quantitative characteristics of Bn–Bs interaction, namely, the effective correlation time  $\tau$  for the monomeric and Bn-complexed Bs and the order parameter  $S$  characterizing spatial angular reorientation of the attached spin label before and after complex formation. Two spin labels attached to the same amino acid residue, C82, were used to obtain reliable data.

## MATERIALS AND METHODS

Spin label 1 (SL1), 3-(2-maleimidoethylcarbamoyl)-2,2,5,5-tetramethylpyrrolidine-1-oxyl, was from Aldrich Chemical Co (USA); spin label 2 (SL2), 4-(2-chloromercuriphenyl)-2,2,5,5-tetramethyl-3-imidazoline- $\Delta^3$ -1-oxyl [10] was synthesized by Dr. A. B. Shapiro. *Escherichia coli* strains TG1 (*hsdR5*, *supE*, *thi*,  $\Delta$ (*lac-pro*), [*F'*, *traD36*, *proA*<sup>+</sup>*B*<sup>+</sup>, *lacI*<sup>q</sup> $\Delta$  M15]), and HB101 (*F*<sup>–</sup>,  $\Delta$ (*gpt-proA*)62, *leuB6*, *glnV44*, *ara-14*, *galK2*, *lacY1*,  $\Delta$ (*mcrC-mrr*), *rpsL20* (Str<sup>r</sup>), *xyl-5*, *mtl-1*, *recA13*) were from the collection of NII Genetika (Moscow, Russia); yeast extract and tryptone were from Difco (USA); chromatography columns and supports were from Amersham Biosciences (Germany). Tris, DTT, and Tween 20 were from Sigma (USA); other reagents were analytical and chemical grade domestic products.

**Protein expression and purification.** To obtain the wild type barnase, *E. coli* strain TG1 was transformed with the pPBn vector (kindly provided by Dr. A. A. Schulga), where *Bn* gene expression was controlled by thermosensitive repressor *cI857*, and Bn was synthesized as a precursor containing STII signal peptide for periplasmic localization at the N-terminal, which is specifically cleaved during Bn secretion into the extracellular medium.

Barnase was isolated and purified according the procedure described by Hartley [11] and Schulga [12] with minor modifications. Colonies from a fresh dish, before they reached  $A_{600, 1\text{cm}} = 0.05$ , were transferred into YTPS nutrient medium (1% yeast extract, 1% tryptone, 80 mM  $\text{K}_2\text{HPO}_4$ , 20 mM  $\text{KH}_2\text{PO}_4$ , 0.9% NaCl, pH 7.4) and cultivated at 37°C overnight. After that they were cooled on ice, supplemented with glacial acetic acid (5%), and stirred on ice for an additional 30 min; then the cells were removed by centrifugation. Phosphocellulose P-11 equilibrated with 20 mM NaOAc, pH 5.0, was added to the supernatant (20 ml per liter of supernatant) and stirred on ice for 2 h; the then supernatant was removed by decanting. The P-11 suspension was washed thrice with 1 liter of 20 mM NaOAc, pH 6.0, by decanting and transferred into a C16/40 column. The column was equilibrated with 20 mM  $\text{NH}_4\text{OAc}$ , 2 mM EDTA, pH 8.0, and barnase was eluted with 20–720 mM concentration gradient of  $\text{NH}_4\text{OAc}$ , (slope 3 M/liter). Virtually pure Bn was eluted with 550–650 mM  $\text{NH}_4\text{OAc}$ . The effluent obtained was diluted 10 times with 20 mM NaOAc, 2 mM EDTA, pH 6.0, and loaded onto a Source 30S column. The column was equilibrated with 10 mM potassium phosphate, 10 mM EDTA, pH 7.0, and Bn was eluted with a 0–300 mM NaCl concentration gradient (slope 1 M/liter) in the same buffer. Pure Bn was eluted at about 150 mM NaCl.

Isolation and purification of Bs was performed according to the procedure described by Dr. I. Protasevich [13] with minor modifications. To get biomass containing Bs C40A, *E. coli* strain HB101 was transformed with the pMT641 plasmid DNA (kindly provided by Dr. R. Hartley). Resulting colonies were transferred into TB medium (3.2% yeast extract, 2.6% tryptone, 90 mM  $\text{K}_2\text{HPO}_4$ , 10 mM  $\text{KH}_2\text{PO}_4$ , 0.9% NaCl, pH 7.5) in the quantity needed to get  $A_{600, 1\text{cm}} = 0.2$ , cultivated at 37°C overnight, and pelleted by centrifugation. Then cells were resuspended in lysis buffer (20 mM Tris, 10 mM  $\text{KH}_2\text{PO}_4$ , 10 mM EDTA, 10 mM DTT, 100 mM NaCl, pH 8.0) and broken by sonication. The lysate was clarified by centrifugation. Nucleic acids were precipitated with 0.04% polyethylenimine, and proteins were fractionated by gradual salting-out with ammonium sulfate. The 40–80% fraction was diluted in lysis buffer and loaded onto a C16/100 column packed with 180 ml of superfine Sephadex G-100 equilibrated with TSDT buffer (20 mM Tris, 20 mM NaCl, 2 mM DTT, 0.05% Tween 20, pH 8.5). Then 115–140 ml of the effluent fraction was loaded onto a HiTrap column packed with Q-Sepharose FastFlow, washed with TSDT and TDG buffers (20 mM Tris, 4 mM DTT, 10% glycerol, pH 8.5), and eluted with 0–1 M NaCl concentration gradient in TDG buffer (slope 10 M/liter). Homogeneous C40A Bs was eluted at 100 mM NaCl.

**Spin labeling of the protein. Introduction of the SL1 spin label into the Bs molecule.** Bs was treated with 50 mM

DTT for 1 h at 4°C, and the excess of DTT was removed on a NAP5 column equilibrated with phosphate buffered saline (PBS) (70 mM K<sub>2</sub>HPO<sub>4</sub>, 30 mM KH<sub>2</sub>PO<sub>4</sub>, 100 mM NaCl, pH 7.2). The effluent (100-μl aliquot, 4 g/liter) was supplemented with 3-fold molar excess (relative to the protein) of SL1 alcohol solution and incubated overnight at 4°C; then the excess label was removed on a NAP5 column equilibrated with PBS. The C40A Bs concentration in the fractions chosen for further analysis was 1.2 g/liter.

#### Attaching of the SL2 spin label to the Bs preparation.

A 120-μl sample of Bs solution in PBS (4 mg/ml) treated with DTT (see above) was supplemented with 3 μl of a label in alcohol solution (15 mg/ml), and after 1–5 min EPR spectra were recorded. SL2 spin label has a high affinity to the thiol groups of proteins [14, 15]. The number of SL2 molecules in the sample was a little less than that of Bs molecules, so after the addition of the spin label aliquot, all SL2 molecules were bound to the Bs protein. Residual unlabeled protein did not affect the final EPR spectrum of the sample.

**Formation of Bn–Bs complex.** To form Bn–Bs complex, Bn and Bs preparations were mixed in equimolar ratio or with a slight excess of Bn that apparently did not influence the final results, considering the EPR follows only the spin labeled protein.

**Registration of EPR spectra and viscosity of solutions.** EPR spectra of samples in solution were recorded on Varian E-104A EPR spectrometer (USA) at HF modulation amplitude of 1 and 2 G and microwave power of 5 mW. The scan range of the magnetic field was 100 and 200 G, and scan time was 8 and 4 min, respectively. EPR spectra of samples frozen at 77 K were recorded at the minimal for this instrument microwave power of 0.2 mW. Temperature was controlled by standard temperature unit V-547 with the accuracy ±0.5°C. Sucrose concentration in the sample was determined with a Zeiss refractometer with the accuracy ±0.2%, the solution viscosity,  $\eta$ , for each temperature was determined with the accuracy not worse than ±0.05 cP using Osmer–Sylvys tables. The distances between the extrema of the EPR spectra were determined with accuracy not worse than ±0.4 G.

**Temperature–viscosity dependences of the EPR spectra.** To extract unambiguous information from experimental EPR spectra of spin labeled macromolecules, it is necessary to decrease by any means the degree of degeneracy of the EPR spectra form in many parameters defining the EPR spectrum. According to this theoretical consideration, it was always emphasized in our articles [3, 6–9, 14–18] that unambiguous consideration could be established only for EPR spectra with broad outer peaks (BOPs). The method is to diminish the temperature activation of a spin label attached to a macromolecule. For that the temperature is decreased until the BOPs appeared, and then their shifts are followed increasing the viscosity of the medium. Therefore, it is

necessary to obtain a series of EPR spectra of spin labeled samples in the solution at constant temperature and different viscosities, and measure the distance  $2A'$  between BOPs in these spectra in Gauss. The designations and terminology referring to the EPR spectra of spin labeled macromolecules as well as their interpretation have been described earlier [3, 6–9]. Plotting the  $2A'$  value on the ordinate axis, and  $(T/\eta)^{0.74}$  value on the abscissa, we get linear dependences for every temperature. These are the so-called temperature–viscosity dependences [6–9] which remain linearity until 8–10 cP (or approximately 40% sucrose, usually used for creating the solution viscosity). At further increase of medium viscosity the condition of fast reorientation of spin label relative to the protein molecule ( $\tau_{\text{label}} < 1$  nsec) is violated, and a positive deviation from linearity for  $2A'$  is observed. The intercept of the straight line with the ordinate axis gives the  $2\bar{A}$  value. The  $2A'$  distance in EPR spectra with BOPs is smaller than the  $2A_{zz}$  distance in the “powder” EPR spectrum. Contribution to this shift is given both by fast motion of a spin label relative to the protein and by slow motion of the protein globule itself in the solution. So the value of the total shift can be represented in the following way:

$$2A_{zz} - 2A' = (2A_{zz} - 2\bar{A}) + (2\bar{A} - 2A') = \Delta_S + \Delta_\tau. \quad (1)$$

The first component depends on the order parameter  $S$ :

$$S = \frac{2\bar{A} - 2a_0}{2A_{zz} - 2a_0} \quad (2)$$

(where  $a_0$  is tensor trace of nitroxyl SFS [6–8]), in other words, on the volume of the angular space assigned by the proximal environment of the protein to all reorientations of the spin label [6–8] (tensor components of SFS for SL1 and SL2 are presented in Table 1). This value depends on temperature: the higher the temperature, the more  $S$  parameter is different from 1. At  $S = 1$  the spin label is strictly attached to the protein (or undergoing axial rotation around the  $Z$  axis). At  $S = 0$  spin label is rapidly spinning around the  $R$  axis, making the magic angle with the  $Z$  axis. In this case, the EPR spectrum consists of three

**Table 1.** Tensor components of nitroxyl SFS in SL1 and SL2 structures

Spin label	$2A_{zz}$ , G	$2a_0$ , G
SL1	71.50	31.80
SL2	69.25	31.30

sharp lines, and this spectral line shape does not depend upon the protein  $\tau$  value. Taking into account formula (2) for the order parameter  $S$ , the first component in (1) can be represented as:

$$\Delta_S = (1 - S) (2A_{zz} - 2a_0). \quad (3)$$

The value of the second component in Eq. (1) gives the shift of broad outer peaks (BOPs) relative to  $2\bar{A}$ . This shift is determined by the effective value of the rotational correlation time  $\tau$  [5-7]:

$$\tau = \frac{a}{S} \left( \frac{\Delta_\tau}{S} \right)^b. \quad (4)$$

Here the  $\tau$  value is measured in nanoseconds, the BOP shift value  $\Delta_\tau$  in G, order parameter  $S$  is a non-dimensional variable (2), and constants  $a = 197$  and  $b = -1.39$ . The  $\tau$  value is effective in the sense that in solution Bs structure itself and in complex with Bn obey the Brownian motion of macromolecules. However, the Stokes–Einstein relation is observed not only for “rigid” macromolecules, but is also true for flexible ones [9].

All  $\tau$  values obtained at 1°C and any solution viscosity are extrapolated to normal conditions (293 K, 1 cP) by means of the Stokes–Einstein relation,  $\tau = V\eta/kT$  (where  $V$  is volume of a hydrated macromolecule,  $\eta$  is viscosity of protein aqueous solution,  $k$  is Boltzmann constant,  $T$  is absolute temperature), and listed in Table 2. The value of  $(\eta/T)^{1/b}$  is plotted on temperature–viscosity dependence graphs, where  $b = -1.39$ , i.e.  $(T/\eta)^{0.74}$ , that follows from the Stokes relation and Eq. (4).

## RESULTS

Before applying the spin label method for any object of investigation, it is first necessary to determine the initial components for both magnetic tensors of nitroxyls in the structure of any spin label. The two spin labels, SL1 and SL2, each containing five-member nitroxyl (SL1, pyrrolidine; SL2, imidazoline), were used in the

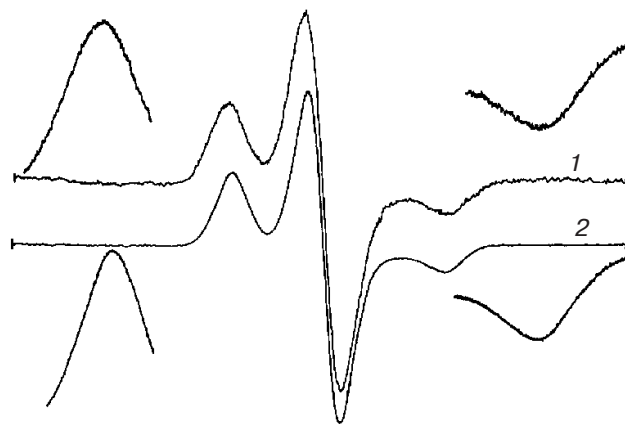


**Fig. 1.** The “powder” EPR spectra of spin-labeled Bs at 77 K: 1) 40% sucrose solution of Bs-SL1 ( $2A_{zz} = 71.5$  G); 2) 40.5% sucrose solution of Bs-SL2 ( $2A_{zz} = 69.25$  G). Both EPR spectra were recorded at scan range of the magnetic field of 200 G. Separately (on the left and on the right) the BOPs used to calculate  $2A_{zz}$  distance at scan range of 100 G are shown.

present study. In Fig. 1, the “powder” EPR spectra of both protein-attached spin labels are shown for buffered protein solutions (with and without sucrose) frozen at 77K. The largest of the three principal components of SFS of nitroxyl, component  $A_{zz}$ , is determined from these spectra as the distance between the broad outer peaks, which is equal to  $2A_{zz}$ . Also from the EPR spectra of free spin label in solution (which has three sharp lines at room temperature) the value of isotropic constant of SFS  $a_0$  is calculated as the distance between the sharp outer peaks equal to  $2a_0$ . Addition to the solution of sucrose to 70% does not influence  $2a_0$  value. These are two very important principal tensor components of SFS of nitroxyl for spin labeled proteins in aqueous solution experimentally measured on EPR spectrometer in the X-band (Table 1). Spin labels attached to exposed protein residues are immersed into the aqueous solution, and therefore magnetic parameters of nitroxyls in the spin labels are determined by the polarity of the aqueous medium that spin labeled proteins are dissolved in. After initial magnetic parameters of the spin labels are defined, it is possible to

**Table 2.** Extrapolated values of  $2\bar{A}$ , order parameter  $S$ , and effective rotational correlation times  $\tau$  for spin labeled proteins

Spin-labeled protein	$2\bar{A}$ , G	$S$ (1°C)	$\tau$ (1°C), nsec	$\tau$ (20°C), nsec
Bs-SL1	$62.1 \pm 0.2$	$0.76 \pm 0.02$	$8.0 \pm 0.8$	$4.0 \pm 0.8$
Bs-SL1–Bn	$69.8 \pm 0.2$	$0.96 \pm 0.02$	$16.0 \pm 0.8$	$9.0 \pm 0.8$
Bs-SL2	$57.8 \pm 0.2$	$0.70 \pm 0.02$	$6.6 \pm 0.8$	$3.0 \pm 0.8$
Bs-SL2–Bn	$63.9 \pm 0.2$	$0.86 \pm 0.02$	$15.6 \pm 0.8$	$8.5 \pm 0.8$



quantitatively process experimental data according to the temperature–viscosity dependence procedure. The requisite condition for this treatment is the presence of BOPs in the EPR spectra. As shown above, for BOPs to appear in EPR spectra of any spin label attached to a protein of fixed molecular weight, it is necessary to decrease the temperature and to increase the viscosity of the sample solution.

In the beginning of the present work, the elongated spin label SL1 was used. Two spectra of Bs-SL1 in solution are shown in Fig. 2a. Spectrum 1 does not contain BOPs at 20°C. On decreasing temperature to 1°C, the EPR spectrum is markedly immobilized (spectrum 2), but, as easily seen, it is not yet enough for BOPs to appear. Certainly, this is connected with the structure of SL1 (which has a long linker for the attachment to the SH-group of cysteine) and to the structure of the nearest interacting with the label protein environment. Both factors lead to weakly immobilized EPR spectra since the decrease in temperature to 1°C does not cause BOPs to

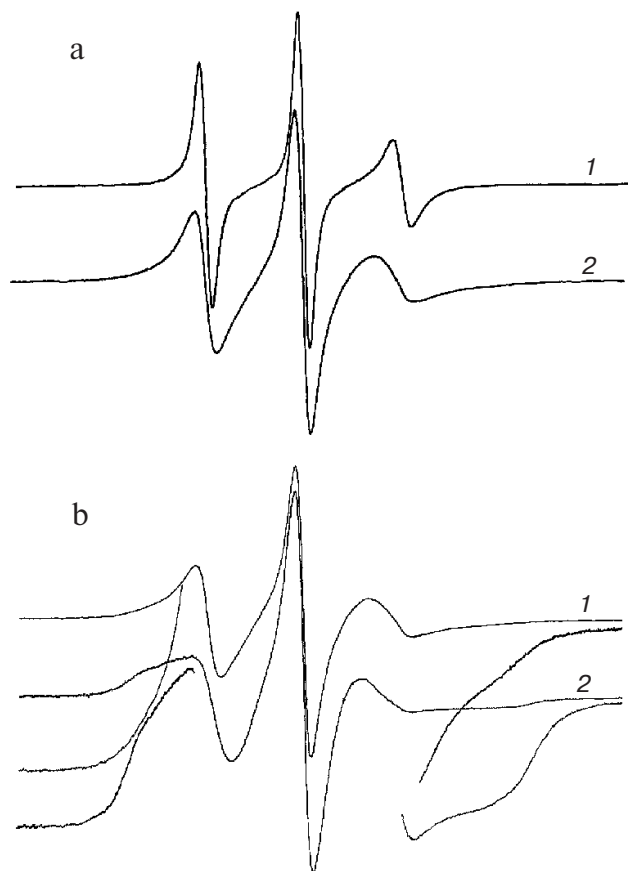


**Fig. 2.** Bs-SL1 EPR spectra as a function of temperature and viscosity: a) at 20°C and 0% sucrose (1) and at 1°C and 0% sucrose (2); b) at 1°C and 6.5% sucrose (1) and at 1°C and 26.5% sucrose (2). Spectra were recorded at scan range of the magnetic field of 100 G. Separately BOPs (left and right) recorded at higher gain are shown for each EPR spectrum.

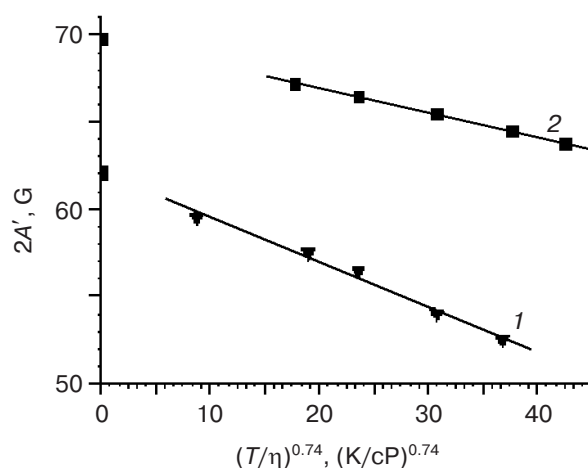


**Fig. 3.** Temperature–viscosity dependences of the  $2A'$  distance between BOPs in the EPR spectra of Bs-SL1 (1) and its complex with Bn (2) at 1°C. Lines are calculated by least square regression. Line 1 crosses the ordinate axis giving the extrapolated value of  $2A = 62.09$  G and line 2 gives  $2A = 69.80$  G.

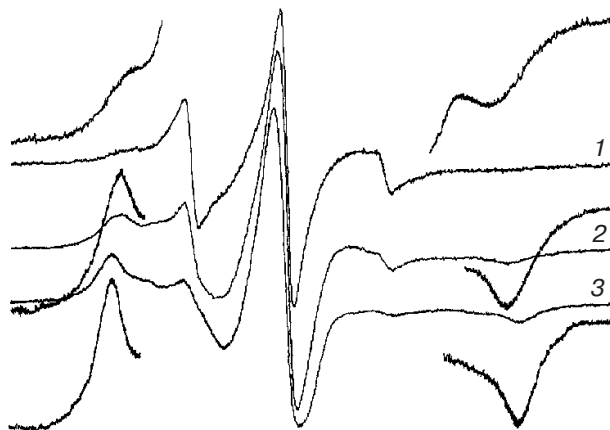


**Fig. 4.** EPR spectra of Bs-SL1–Bn complex: 1) at 20°C and 0% sucrose; 2) at 1°C and 0% sucrose; 3) at 1°C and 28% sucrose. BOPs recorded at higher gain are shown for each EPR spectrum. Scan range of the magnetic field, 100 G.

appear. With the increase of medium viscosity at 1°C (Fig. 2b), beginning from 6.5% sucrose, BOPs are already observed (spectrum 1) in the form of a smoothed line with inflection. At 23% sucrose (spectrum 2), BOPs are distinctly seen (lines with inflection) both on the left (low magnetic field) and on the right (high magnetic field) side of the spectrum. Hence, BOPs in the EPR spectra of Bs-SL1 are observed, but with no evident extrema. However, the distance between BOPs,  $2A'$ , can be assessed using the inflection points at these peaks, and plotting the temperature–viscosity graph shown in Fig. 3 (line 1), and also the effective rotational correlation time for Bs-SL1 can be determined, which is 4 nsec.

Special attention should be given to whether Bs-SL1 gives EPR spectra without obvious extrema, so in Bs-SL1–Bn complex they show up quite clearly (Fig. 4). This is a very interesting fact whose occurrence depends exclusively upon the label structure. The EPR spectral line shape is sharply changed towards strong immobilization, i.e. distinct BOPs appear. In other words, the interaction of the two protein molecules leading to its tight contact results in the BOPs extrema become notable even at 20°C (spectrum 1). At 1°C (spectrum 2) the BOPs appear with increasing amplitude and are well observed both at low and high magnetic field with rather well-defined extrema between which distance  $2A'$  is measured. Spectra 1 and 2 correspond to the samples without sucrose (0%), and spectrum 3 corresponds to the sample containing 28% sucrose. All  $2A'$  experimental points (some of them are listed in Fig. 4) for the corresponding Bn–Bs-SL1 sample viscosities are presented on the corresponding temperature–viscosity dependence graph (Fig. 3, line 2). The slope of this line to the abscissa axis is used to determine the effective rotational correlation time of the Bs-SL1–Bn protein complex, which is 9 nsec (Table 2).

Thus, using spin label SL1 a qualitatively well-defined picture was obtained: rotational correlation times and order parameters for Bs-SL1 alone and in complex with Bn were determined. For the confirmation (or denial) of these data, we used another spin label, SL2 (with shorter linker), which as known gives evidently expressed BOPs under interaction with the proximal protein environment and attached to the same SH-group of Bs [14, 15].

In Fig. 5, EPR spectra of Bs-SL2 at 1°C are shown. As seen, even without sucrose BOPs with definite extrema appear (Fig. 5, 1). The high field BOP is well shaped, but the low field peak is half-resolved. After addition of sucrose to 6% the low field peak (Fig. 5, 2) becomes well-resolved too. Further increase of the viscosity of the spin labeled protein solution by adding sucrose to 16 and 19.5% (Fig. 5, 3 and 4) leads to even more well-defined extrema of BOPs, which allows plotting a linear temperature–viscosity dependence (Fig. 6, 1) and determining  $\tau = 3.0 \pm 0.8$  nsec and order parameter  $S = 0.70$  (Table 2) with higher accuracy.

In accordance with the main aim of the present study, it should be determined how the EPR spectra of Bs-SL2 would be changed upon formation of the Bn–Bs-SL2 complex. The EPR spectra are presented in Fig. 7. As seen, the formation of the complex of the two proteins leads to EPR spectral change sharply difference compared to the spectra in Fig. 5 and become “strongly immobilized” and very close to each other, differing only in the shift of BOPs from the center of the spectrum. That is why only two spectra are shown in Fig. 7: at 20 and 1°C. The temperature–viscosity dependence for the distances between BOPs at 1°C is shown in Fig. 6 (line 2). The slope of this line gives  $\tau = 8.5$  nsec, and its intersection

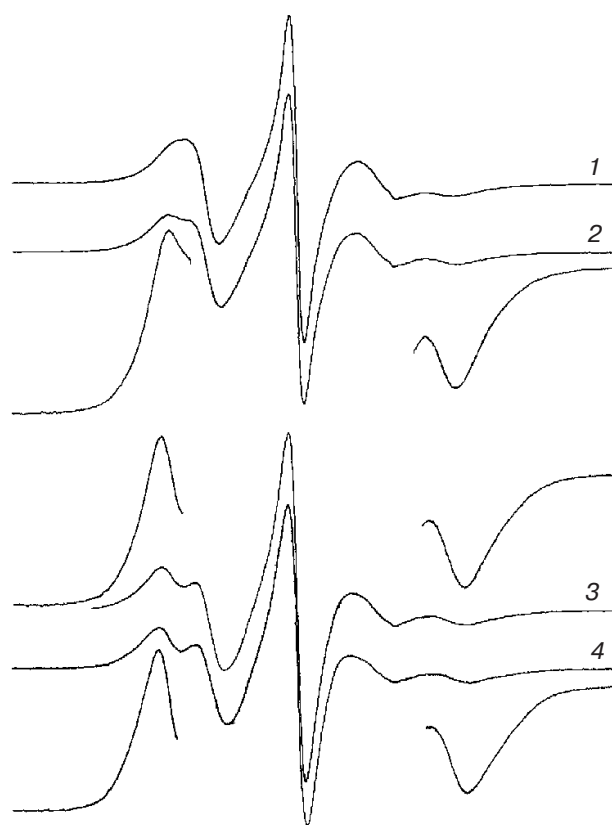


Fig. 5. Bs-SL2 EPR spectra at 1°C and variable viscosity (sucrose concentration, %): 1) 0; 2) 6; 3) 16; 4) 19.5. BOPs (at higher gain) are shown for each EPR spectrum where they are present. Magnetic field, 100 G.

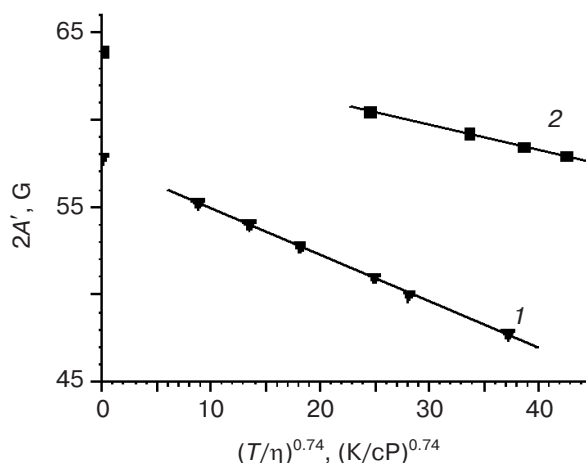


Fig. 6. Temperature–viscosity dependences of the distances  $2A'$  between BOPs in the EPR spectra of Bs-SL2 (1) and of its complex with Bn (2) at 1°C. Lines are calculated by least square regression. Line 1 crosses the ordinate axis giving the extrapolated value of  $2\bar{A} = 57.80$  G, and line 2 gives  $2\bar{A} = 63.92$  G.

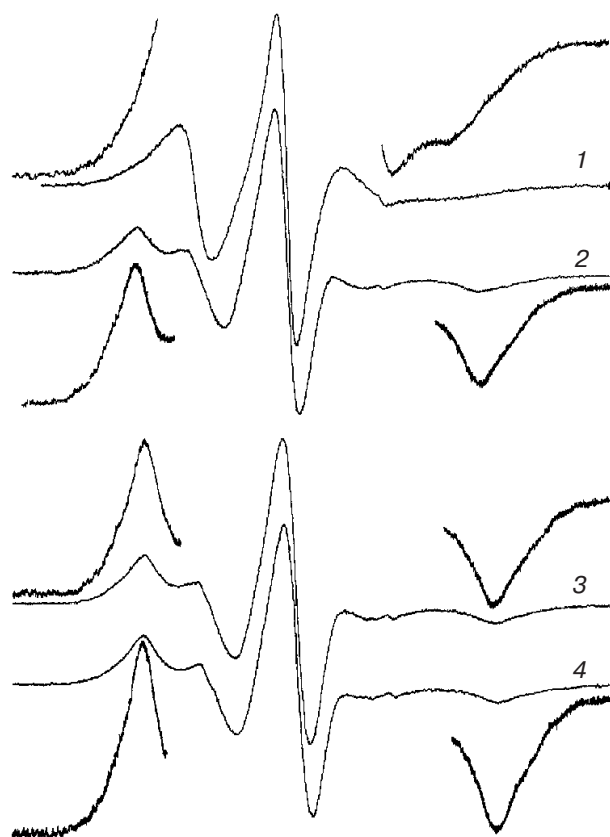


Fig. 7. EPR spectra of Bs-SL2-Bn complex: 1) at 20°C and 0% sucrose; 2) at 1°C and 0% sucrose; 3) at 1°C and 4.5% sucrose; 4) at 1°C and 10% sucrose. BOPs recorded at higher gain are shown for each EPR spectrum. Scan range of the magnetic field, 100 G.

point with ordinate axis 2A gives order parameter  $S = 0.86$  calculated according to Eq. (2). The results of quantitative processing of EPR spectra of the spin labeled samples are presented in Table 2. Therefore, we have a completed analogy of the behavior of the two Bs-attached spin labels in the individual labeled Bs and in its complex with Bn. How both labels are informative of local dynamics of Bs in complex with Bn will be considered below.

## DISCUSSION

The initial point of the discussion is that both spin labels SL1 and SL2 bind to the same thiol group of Cys82 residue of barstar having molecular weight 10.3 kD. First, the experiment on temperature-viscosity dependence of BOPs in EPR spectra was performed for SL1 and then for SL2. It was found that Bs-SL1 spectra did not contain explicitly defined extrema (Fig. 2), so the assessment of BOP positions was made using inflection points. The slope of the line in Fig. 3 (1) gives the rotational correlation time value of the carrier brought to normal condi-

tions (20°C and 0% sucrose, correspondent to the viscosity of solution of about 1 cP) equal to 4 nsec. Starting from the molecular weight of Bs, the theoretical value of rotational correlation time for it should be:

$$20 \text{ nsec} \cdot 10.3 \text{ kD}/50 \text{ kD} = 4.1 \text{ nsec},$$

considering that the rigid molecule with molecular weight of 50 kD is rotating in the solution at normal conditions with  $\tau = 20$  nsec (Stokes law) [6-9]. Then Bs-SL1 was added to Bn and the temperature-viscosity dependence (Fig. 3, 2) was determined again using the EPR spectra with well-defined BOPs (Fig. 4). As a result the correlation time  $\tau = 9$  nsec for the rigid molecule with molecular weight of:

$$10.3 \text{ kD} + 12.4 \text{ kD} = 22.7 \text{ kD},$$

where 12.4 kD is the molecular weight of Bn. It should be noted that also in this case very good agreement with the Stokes equation is observed:

$$\tau = 20 \text{ nsec} \cdot 22.7 \text{ kD}/50 \text{ kD} = 9.1 \text{ nsec}.$$

Consequently, it is possible to say that the complex between Bs-SL1 and Bn is quite tight. The label is located near the contact site of two halves of the complex, and does not disturb the protein-protein interaction; at the same time (quasi falling into the force field formed between two subunits), its mobility is affected by spatial restrictions due to the formation of the close contact between the two proteins. As a result, the order parameter  $S$  approximates 1, and the correlation time  $\tau$  corresponds to the molecular weight of the whole Bs-Bn complex for the rigid molecule. The nitroxyl of SL1 is situated on the boundary of the subunits, even though it can experience fast oscillations with order parameter of 1 around the Z axis.

For spin label SL2 the conclusion about a stable complex between modified spin labeled Bs and Bn is confirmed. The EPR spectra of Bs-SL2 (Figs. 5 and 7) already have obviously expressed BOP extrema, and the temperature-viscosity dependence is determined from these resolved extrema, instead of using inflection points as for spectra of Bs-SL1. It appears that in the case of Bs-SL2 the correlation time  $\tau = 3$  nsec (not 4 nsec), which is within the limits of an experimental error of  $\pm 0.8$  nsec. For the complex Bs-SL2-Bn,  $\tau$  and  $S$  values were 8.5 nsec and 0.86, respectively.

Here we would like to discuss the parameter  $\tau$  for the Bn molecule, as well as for Bs, whose theoretical value should be:

$$20 \text{ nsec} \cdot 12.4 \text{ kD}/50 \text{ kD} = 5.0 \text{ nsec}.$$

Since the correlation time and volume (molecular weight) of a molecule according to Stokes law are direct-

ly proportional, based on our data, having determined  $\tau = 4$  nsec for the Bs molecule and  $\tau = 9$  nsec for that of its complex with Bn (Table 2), we calculate 5 nsec. Recently [19], the  $\tau$  value for  $^{15}\text{N}$ -labeled Bn was determined by NMR using a complex analysis of two-dimensional  $^{15}\text{N}$ - $^1\text{H}$  correlation NMR spectra. The authors reported  $\tau = 5.56 \pm 0.01$  nsec, which is in good agreement with our estimation.

It is interesting that the SL1 nitroxyl (with the more lengthy linker) in the complex with Bn has a value of order parameter  $S$  closer to 1 than for the SL2 nitroxyl (with fewer chemical bonds) (Table 2). Hence, it is possible to tell that the spin label SL2 hits another area of force field upon binding of the two proteins.

Spin label SL1 attached to Bs has order parameter  $S = 0.77$ , which increases to 0.96 (i.e. almost to 1) upon the formation of the Bs–SL1–Bn complex (Table 2). Therefore, after specific protein–protein interaction of Bs–SL1 and Bn, the C82 residue together with the spin label is so immobilized, or its possible reorientations are so limited, that nitroxyl spin label only undergoes the rotation around its molecular axis  $Z$ . In the case of Bs–SL2, the order parameter  $S = 0.70$  increases to 0.86 (that is also close to 1) (Table 2) upon the formation of the Bs–SL2–Bn complex.

Thus, spin labels SL1 and SL2, different in their chemical structures, when attached to Bs protein through the same Cys82 residue demonstrate similar dynamic behavior upon the formation of the Bs–Bn complex. It is clearly estimated from the comparison of the two temperature–viscosity dependences (Figs. 3 and 6) for Bs–SL and for Bs–SL–Bn. Both figures have identical scales on both axes. It is easy to see that line slopes for Bs labeled with the different labels are identical, and slopes for the Bs–Bn complex are identical too. This is not surprising since this slope is defined by the rotational correlation time of protein globule and does not depend on the type of spin label attached. Nevertheless, values of order parameters depend on the type of spin label (extrapolated  $2\bar{A}$  values are different in Figs. 3 and 6) and demonstrate (Table 2) that spin label SL1, having more bonds, is immobilized stronger by the protein structure (contact site of the two proteins) than spin label SL2, which has a smaller number of bonds. The protein environment apparently accessible for spin label SL1 limits angular reorientation of nitroxyl more strongly than that for the spin label SL2 nitroxyl.

The three-dimensional structure of Bs–Bn complex (Fig. 8) conforms to these conclusions. In this figure it is seen that the  $C_\alpha$  carbon of the C82 residue is located on a periphery of the contact site of the interacting proteins, and therefore its alkylation with a spin label should not disturb complex formation. The data of the dynamic spin label method provided evidence for this. Bs, spin labeled at C82, forms a strong Bs–SL–Bn complex, with values of rotational correlation time of  $9.0 \pm 0.8$  nsec for SL1 and  $8.5 \pm 0.8$  nsec for SL2. The “strong complex” term means

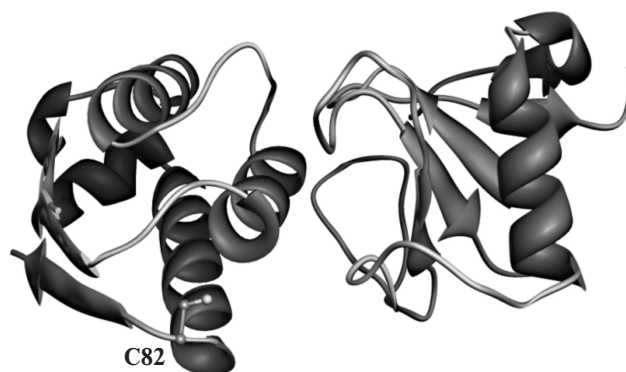


Fig. 8. Spatial structure of Bs–Bn complex (PDB ID 1b2s). Barstar residue C82, alkylated with spin label, is indicated.

EPR spectrum registration time is much less than the lifetime of the complex. Hence, introduction of spin labels at C82 does not attenuate the complex formation.

Quantitatively the correlation time corresponds to a rigid structure of Bs–Bn complex consisting of two proteins with molecular weights of 10.3 and 12.4 kD, respectively. At the same time, the spin labeled Bs molecule has rotational correlation time of  $4.0 \pm 0.8$  nsec for SL1 and  $3.0 \pm 0.8$  nsec for SL2, that also points to a protein molecule with a rigid structure. It is known that Bs itself forms dimers at concentrations of about 2 mg/ml [20]. Indeed, using spin label SL2 we observed a weak dimerization effect at the same concentrations of Bs. However, this in no way influences the final result.

So, it appears that correlation times of spin labeled Bs in solution and Bs–Bn molecular complex exactly correspond to the molecular weight of these objects. Here, order parameter  $S$  is sharply increased almost reaching 1: from 0.76 to 0.96 and from 0.70 to 0.86 for SL1 and SL2, respectively. According to the above-described method of interpretation of EPR spectra, the first result demonstrates that the structures of Bs and Bn are “rigid” entities, and the second result provides evidence about the strong restriction of mobility of both spin labels (located on the boundary of the Bs–Bn contact site) from the nearest to spin label environment in the contact site of these two proteins.

This work was performed with financial support of the Russian Foundation for Basic Research (grants 07-02-00649-a and 06-04-49686-a), SNF IB73A0-110842/1, and the program “Molecular and Cell Biology” with the financial support of the Presidium of the Russian Academy of Sciences.

## REFERENCES

1. Hartley, R. W. (1997) in *Ribonucleases. Structures and Functions* (D'Alessio, G., and Riordan, J. F., eds.) Academic Press, N. Y., pp. 51–100.



2. Berliner, L. (1979) *Spin Labeling. Theory and Applications* [Russian translation], Mir, Moscow.
3. Timofeev, V. P., and Tsetlin, V. I. (1983) *Biophys. Struct. Mech.*, **10**, 93-104.
4. Deev, S. M., Waibel, R., Lebedenko, E. N., Schubiger, A. P., and Pluckthun, A. (2003) *Nature Biotechnol.*, **21**, 1486-1492.
5. Wong, K. B., Fersht, A. R., and Freund, S. M. (1997) *J. Mol. Biol.*, **268**, 494-511.
6. Timofeev, V. P. (1986) *Mol. Biol. (Moscow)*, **20**, 697-711.
7. Timofeev, V. P., and Samarianov, B. A. (1993) *Appl. Magn. Reson.*, **4**, 523-539.
8. Timofeev, V. P., and Samarianov, B. A. (1995) *J. Chem. Soc. Perkin Trans.*, **2**, 2175-2181.
9. Timofeev, V. P., Tkachev, Ya. V., Novikov, V. V., Varlamova, E. Yu., and Lapuk, V. A. (2005) *Biofizika*, **50**, 787-792.
10. Shapiro, A. B., Volodarsky, L. B., Krasochka, O. N., Avtomyan, L. O., and Rozanzev, E. G. (1979) *Dokl. Akad. Nauk SSSR*, **248**, 1135-1139.
11. Hartley, R. W., and Rogerson, D. L., Jr. (1972) *Prep. Biochem.*, **2**, 229-242.
12. Schulga, A., Kurbanov, F., Kirpichnikov, M., Protasevich, I., Lobachov, V., Ranjbar, B., Chekhov, V., Polyakov, K., Engelborghs, Y., and Makarov, A. (1998) *Protein Eng.*, **11**, 775-782.
13. Protasevich, I. I., Schulga, A. A., Vasilieva, L. I., Polyakov, K. M., Lobachov, V. M., Hartley, R. W., Kirpichnikov, M. P., and Makarov, A. A. (1999) *FEBS Lett.*, **445**, 384-388.
14. Timofeev, V. P. (1983) *Mol. Biol. (Moscow)*, **17**, 519-531.
15. Arutyunyan, A. E., Dudich, I. V., and Timofeev, V. P. (1988) *Mol. Biol. (Moscow)*, **22**, 1045-1061.
16. Dudich, I. V., Timofeev, V. P., Volkenshtein, M. V., and Misharin, A. Yu. (1977) *Mol. Biol. (Moscow)*, **11**, 685-693.
17. Dudich, I. V., Dudich, E. I., and Timofeev, V. P. (1980) *Mol. Immunol.*, **17**, 1335-1339.
18. Timofeev, V. P., Dudich, E. I., and Volkenstein, M. V. (1980) *Biophys. Struct. Mechan.*, **1**, 41-49.
19. Korchuganov, D. S., Gagnidze, I. E., Tkach, E. N., Schulga, A. A., Kirpichnikov, M. P., and Arseniev, A. S. (2004) *J. Biomol. NMR*, **30**, 431-442.
20. Korchuganov, D. S., Nolde, S. B., Riebarkh, M. Ya., Orekhov, V. Yu., Schulga, A. A., Ermolyuk, Ya. S., Kirpichnikov, M. P., and Arseniev, A. S. (2001) *J. Am. Chem. Soc.*, **123**, 2068-2069.